

Electronic Supplementary Information

Dynamics and phase behavior of metallo-dielectric rod-shaped microswimmers driven by alternating current electric field

Suvendu Kumar Panda^a, Srikanta Debata^a, Nomaan Alam Kherani^{a,‡}, and Dhruv Pratap Singh^{a,*}

^a*Department of Physics, IIT Bhilai, Kutelabhata, Durg, Chhattisgarh, 491002, India.*

[‡]*On internship from Department of EE, IIT Bhilai, Kutelabhata, Durg, Chhattisgarh, 491002, India.*

*Corresponding Author: dhruv@iitbhilai.ac.in

1. Guide to supplementary videos

Video S1: The video shows the ICEP motion of Janus microswimmers in the presence of an AC electric field at 10 kHz and 416 kV m⁻¹. The video plays at 1X speed.

Video S2: The Video shows the standing behavior of Janus microrods above 90 kHz at 366 kV m⁻¹. The video plays at 1X speed.

Video S3: The video shows the phenomenon of clustering at low frequency (1 kHz) with 366 kV m⁻¹. The video plays at 4X speed.

Video S4: The Video shows the frequency-dependent phase transition of the Janus rods, starting from the clustering phase to the standing phase at 366 kV m⁻¹. The video plays at 4X speed.

2. Supplementary figure description

2.1. Formation of the monolayer by Langmuir-Blodgett deposition technique:

The first and foremost step before the growth of microrods is to create the closed-packed monolayer of silica beads. To accomplish the task, we adopted the LB deposition technique to form a monolayer of silica beads over a piranha-cleaned silicon wafer surface.¹⁻³ To obtain this, the aqueous solution of commercially available 1µm silica beads (Sigma Aldrich) was initially taken in the desired amount in a centrifuge tube and dispersed in the ethanol solution after the water replacement. Subsequently, a few drops of allyl tri-methoxy silane were added to the solution and subjected to the orbital shaker for 3 hours to render the surface amphiphilic, exhibiting both polar and non-polar characteristics. This crucial step is performed to modify

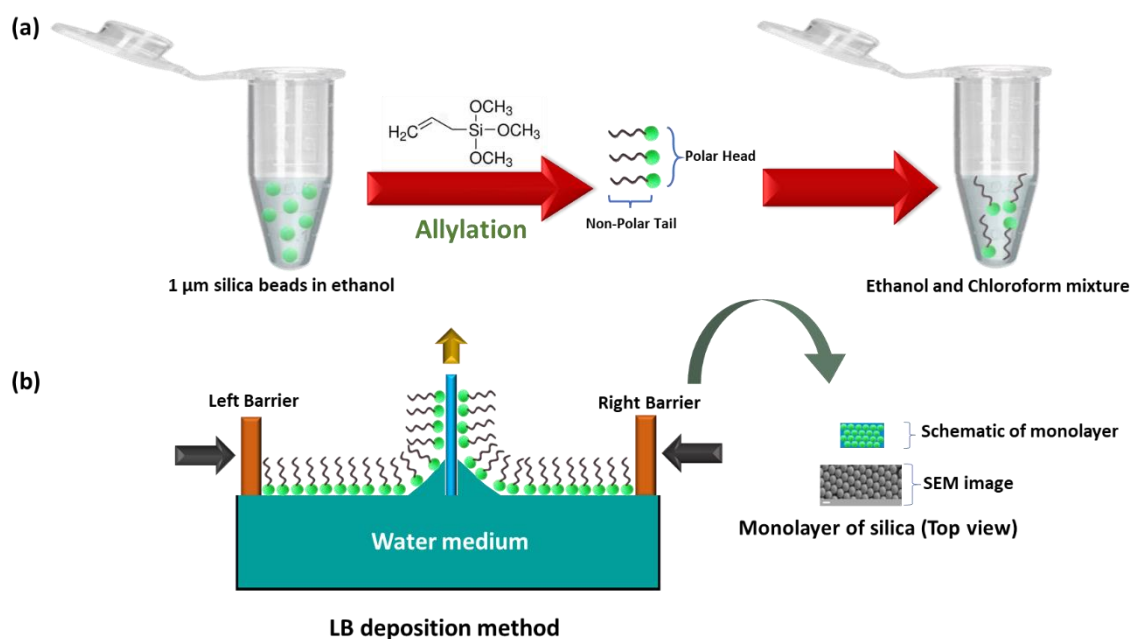


Fig. S1 The monolayer formation process by Langmuir Blodgett (LB) deposition technique. (a) The silica beads are dispersed in ethanol, followed by the allylation to make the beads amphiphilic. Finally, it is contained in a mixture of ethanol and chloroform (1:4). (b) Functionalized silica beads are put in the LB system to grow the closed-packed monolayer of silica. The inset on the right side represents the top view of the obtained monolayer, as shown in the schematic and from the SEM image. The Scalebar shows 1 μm.

the surface properties, facilitating the beads to adhere to the water surface without undergoing sedimentation. Following surface modification, the functionalized beads are placed in a mixture of ethanol and chloroform in a 1:4 ratio. A sequential representation of this procedure is illustrated in **Fig. S1a**. As the monolayer was aimed to coat upon a silicon wafer (100 plane), it was treated with the piranha solution (3 parts of H_2SO_4 : one part of H_2O_2) to keep the surface free from contaminants. The cleaned wafer was then submerged in the water-filled LB trough, and the system was operated to exhibit barrier compression and relaxation to clean up the water surface. After properly visualizing the water surface, the prepared solution of silica beads was slowly spread over the surface of the LB trough with the help of a microliter syringe (Hamilton). Subsequently, we allowed the beads to form a closed-packed single layer over the trough with the adjustment of barrier compression and relaxation speed and by monitoring the surface pressure of the water level. Once the desired pressure was established, the LB system was commanded to act for the deposition by slowly raising the silicon wafer with the motorized dipper stand while keeping the surface pressure of 20 mN m^{-1} throughout the process. A schematic is displayed in the left part of **Fig. S1b** to understand the process. The confirmation

of a closed-packed monolayer was characterized via the SEM image, whose top view is given towards the end of **Fig. S1b**.

2.2. Particle size distribution:

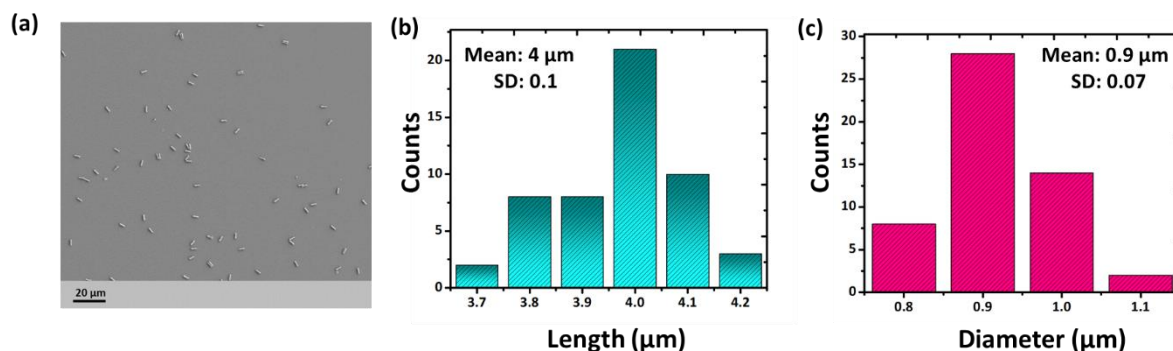


Fig. S2 Measurement of the size of the Janus rods. (a) SEM image shows the distribution of the rods over the surface of the silicon wafer. (b) Histograms of the length and (c) diameter of the Janus rods as measured from the SEM images.

2.3. Fabrication of experimental cell:

The schematics of the fabrication of the experimental cell used to study metallo-dielectric Janus microrods under an AC electric field are shown in **Fig. S3**.

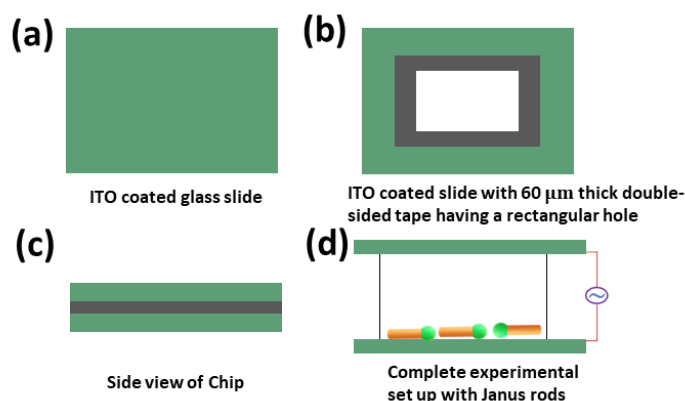


Fig. S3 Schematic representation of experimental cell. (a) ITO coated glass slide. (b) 60 μm double sided tape is used as a spacer for holding the aqueous solution of Janus rods. (c) Side view of microfluidic chip formed by two parallel ITO slides and double-sided tape. (d) Connection of experimental cell to the AC source (function generator).

2.4. Approximation of configuration of Janus rod:

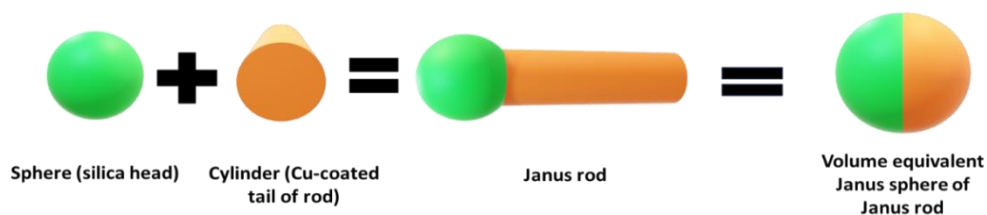


Fig. S4 Schematic shows that the combination of sphere and cylinder takes the configuration of Janus rod, which is equivalent to a sphere of equal volume to that of the rod.

The rod-like structure of the microswimmers possesses the seed layer of a silica sphere of radius r (serving as the head of the rod) and an elongated Cu-coated arm (cylindrical tail of length h and circular face of radius y). So, we have taken it as a combination of the two, as shown in **Fig S4**. This simplified assumption equates the volume of the combination of both segments to the volume of a sphere of radius R .

The diameter of the silica sphere is given as $1 \mu\text{m}$.

The average length and diameter of the cylindrical arm are $3 \mu\text{m}$ and $0.9 \mu\text{m}$, respectively.

If the diameter of the volume equivalent sphere is d , then it can be written as $d = \left(\frac{6V}{\pi}\right)^{\frac{1}{3}}$

$$; \text{ where } V = \pi y^2 h + (4/3) \pi r^3$$

Upon calculating the above formula, the size of the volume equivalent sphere is $1.6 \mu\text{m}$.

2.5. Tracks from a common origin:

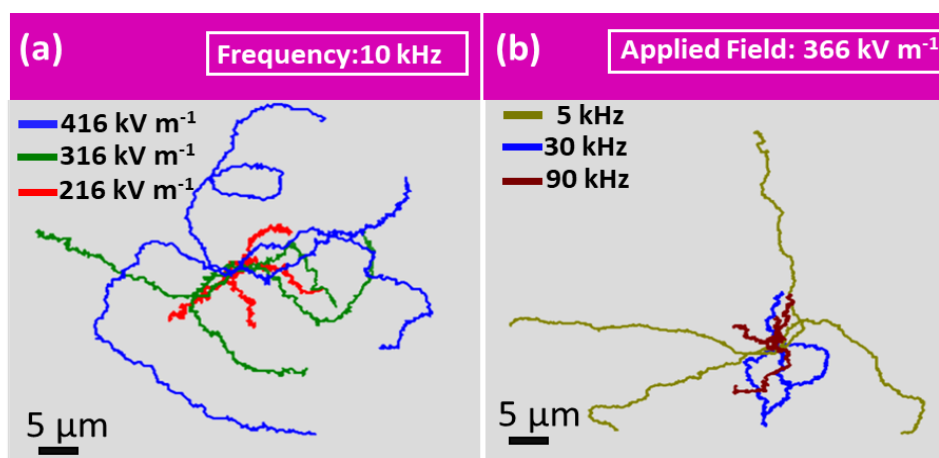


Fig. S5 (a) The trajectories of Janus microswimmers taken for the three different values of applied electric field strength from a common center point at 10 kHz and (b) for three different frequencies at 366 kV m⁻¹, respectively.

To show the random path of the microswimmers during motion, they are characterized for three different field parameters at constant frequency (**Fig. S5a**) and three different frequencies at constant Electric field strength (**Fig. S5b**). The swimmers' tracks are represented from the center (0,0) of the XY coordinate system. Each colored line illustrates the swimmers' motion recorded for varying parameters such as the frequency at const. E-field and vice versa.

2.6. Characterization of Brownian motion of Janus rods:

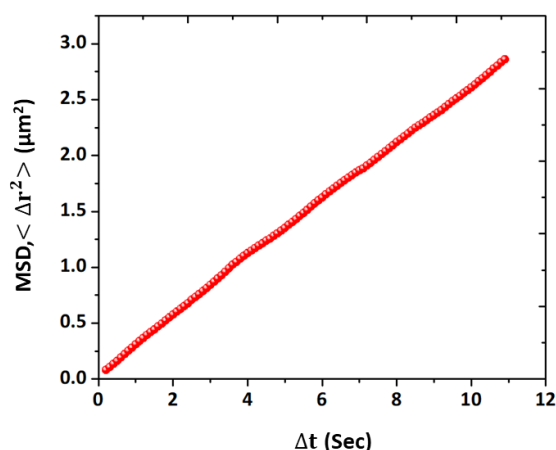


Fig. S6 Experimental MSD plot for Janus rods with no Field (Brownian motion). The measured value of diffusion coefficient ($\langle \Delta r^2 \rangle / 4\Delta t = D_0$) is obtained to be $0.058 \mu\text{m}^2 \text{sec}^{-1}$.

2.7. Characterization of reorientation time of Janus rods:

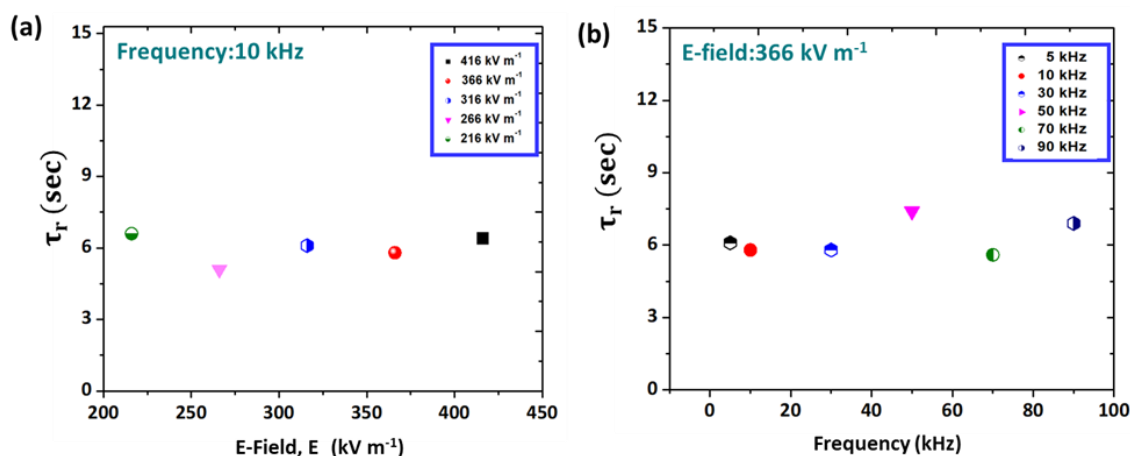


Fig. S7 Reorientation time of rod-like Janus colloids. (a) Reorientation time for different strengths of the Electric field at const. frequency value (10 kHz), and (b) for different frequency values at const. field strength (366 kV m^{-1}).

2.8. Frequency-dependent Phases of Janus rods:

The Janus microrods can be well reconfigured by changing the AC frequency. To get the frequency-responsive phases of these rods, the frequency was initially set at the lower frequency at 800 Hz to favor the cluster formation. Starting from this phase, when the frequency was increased above 800 Hz, these rods dissolved from the cluster phase and slowly migrated randomly in the bounded aqueous medium via ICEP. Keeping this condition for a few seconds and further going towards the higher frequency regime promoted the sliding of the rods from the horizontal to the vertical position. Above a characteristic frequency (90 kHz), they switched their state to a vertically standing position and locked themselves in this

configuration. An event of temporal change of phase transition is presented in **Fig. S8** in a clockwise manner at const. field strength (366 kV m^{-1}).

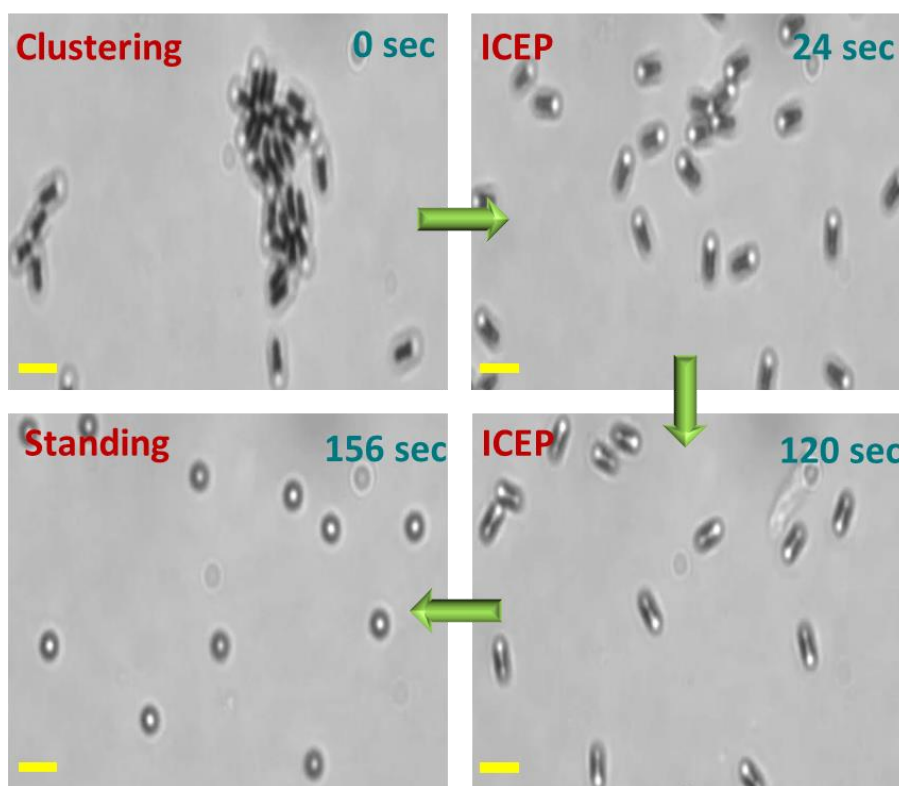


Fig. S8 Switching of different phases of microrods from clustering (Low frequency) to standing (High frequency). The scalebar indicated $4 \mu\text{m}$.

3. References:

- 1 D. Schamel, M. Pfeifer, J. G. Gibbs, B. Miksch, A. G. Mark and P. Fischer, *J. Am. Chem. Soc.*, 2013, **135**, 12353–12359.
- 2 J. Hur and Y.-Y. Won, *Soft Matter*, 2008, **4**, 1261–1269.
- 3 P. Chattopadhyay, L. Wang, A. Eychmüller and J. Simmchen, *J. Chem. Educ.*, 2022, **99**, 952–956.